eNeuro

Research Article: New Research | Cognition and Behavior

Spatial Binding Impairments in Visual Working Memory following Temporal Lobectomy

https://doi.org/10.1523/ENEURO.0278-21.2022

Cite as: eNeuro 2022; 10.1523/ENEURO.0278-21.2022

Received: 17 June 2021
Revised: 22 January 2022
Accepted: 30 January 2022

Spatial Binding Impairments in Visual Working Memory following Temporal Lobectomy

Mamdouh Fahd Alenazi[1,2], Haya Al-Joudi[2], Faisal Alotaibi[2], Martyn Bracewel[1,3,4], Neil M. Dundon[5,6], Mohammad Zia Ul Haq Katshu[7,8], Giovanni d'Avossa[1]

[1] School of Psychology, Bangor University, Bangor, United Kingdom.

[2] Department of Neurosciences, King Faisal Specialist Hospital and Research Centre, Riyadh, Saudi Arabia.

[3] School of Medical Sciences, Bangor University, Bangor United Kingdom.

[4] Walton Centre NHS Foundation Trust, Liverpool, United Kingdom.

[5] Department of Psychological and Brain Sciences. University of California Santa Barbara, Santa Barbara, United States of America.

[6] Department of Child and Adolescent Psychiatry, Psychotherapy and Psychosomatics, University of Freiburg, 79104 Freiburg, Germany.

[7] Division of Psychiatry and Applied Psychology, School of Medicine, University of Nottingham, Nottingham, United Kingdom.

[8] Nottinghamshire Healthcare NHS Foundation Trust, Nottingham, United Kingdom

Corresponding author:
Giovanni d'Avossa, MD
Brigantia Building
College Road
Bangor University
Bangor, Gwynedd LL57 2AS
United Kingdom
Email: g.davossa@bangor.ac.uk

Acknowledgments

Acknowledgements. M.F.A. was supported by a doctoral scholarship from the Organ Transplant Centre at King Faisal Specialist Hospital & Research Centre in Riyadh, Saudi Arabia.

Abstract

Disorders of the medial temporal lobe (MTL) adversely affect visual working memory (vWM) performance, including feature binding. It is unclear whether these impairments generalise across visual dimensions or are specifically spatial. To address this issue, we compared performance in two tasks of thirteen epilepsy patients, who had undergone a temporal lobectomy, and fifteen healthy controls. In the vWM task, participants recalled the color of one of two polygons, previously displayed side by side. At recall, a location or shape probe identified the target. In the perceptual task, participants estimated the centroid of three visible disks. Patients recalled the target color less accurately than healthy controls because they frequently swapped the non-target with the target color. Moreover, healthy controls and right temporal lobectomy patients made more swap errors following shape than space probes. Left temporal lobectomy patients, showed the opposite pattern of errors instead. Patients and controls performed similarly in the perceptual task. We conclude that left MTL damage impairs spatial binding in vWM, and that this impairment does not reflect a perceptual or attentional deficit.

Significance Statement

This study examined color recall in temporal lobectomy patients and healthy controls, to determine whether patients show differential impairments binding color and shape vs color and location of memorised objects. Left temporal lobectomy patients were less accurate recalling color, especially when the target object was identified by the location, rather than the shape it had in the initial display. We found no group difference in a task, which required estimating the centroid of three circles, indicating that the memory impairment was not accounted by perceptual or attentional difficulties. Our findings indicate that lateralised medial temporal circuits are crucial for binding visual features to the location where they had appeared, thus ensuring the primacy of space in organising declarative memories.

Introduction

The role of the medial temporal lobe (MTL) in episodic memory is well established (Squire, 2009). Despite initial reports of preserved immediate memory span in temporal lobectomy patients (Drachman and Arbit, 1966), later studies found that MTL lesions also engender substantial working memory (WM) deficits (Olton *et al.*, 1979; Holdstock *et al*, 1995; Hannula *et al.*, 2006). Which WM processes are specifically supported by the MTL is, nevertheless, a matter of ongoing investigations.

An early, seminal model suggested that visual WM (wWM) contains few discrete "slots", each used to store one and only one object with high fidelity (Luck and Vogel, 1997; Zhang and Luck, 2008). Despite its simplicity, the slot model makes non-trivial predictions. First, the complexity of memorised objects should not affect recall accuracy. Second, recalling feature conjunctions should carry no additional cost over remembering features, since features are stored *ipso facto* as parts of an object into vWM. Wheeler and Treisman (2002) found, instead, that simple objects were recalled more accurately than complex ones, and that recall accuracy was equalised for displays containing the same number of color features rather than the same number of objects. They concluded that memory limitations reflect feature rather than object-based storage mechanisms. Moreover, observers were worse at detecting changes of feature conjunctions than features, indicating that conjunctions are stored or recalled less efficiently than features. Later studies confirmed that changes in feature conjunctions are poorly detected (Allen *et al*., 2006), leading to the suggestion that dimensionally specific registers store features, while an "episodic buffer" is dedicated to holding bound object representations in vWM (Baddeley *et al.*, 2011). The need for binding processes follows logically from the alternative model of vWM which proposes that visual features are stored in dimensionally specific, limited resolution stores (Alvarez and Cavanagh, 2004; Smyrnis *et al*., 2005; Bays *et al.*, 2009). Clearly, if different feature

dimensions are stored separately, then a binding process is required to ensure that features belonging to the same object, but different feature dimensions, are identified as such (Wheeler and Treisman, 2002; Smyrnis *et al.*, 2005).

While the idea that conjunctive binding is required to preserve object identity is not unanimously shared (e.g. Luck and Vogel, 2013), there are several proposals regarding its nature. Treisman and Zhang (2006) concluded that binding is automatic, established initially by the features' shared location, but then becomes location independent. Schneegans and Bays (2017) proposed instead that location information is always required, because features from different visual dimensions are stored in separate retinotopic maps.

Investigators examining the neurological underpinnings of declarative memory largely embrace the idea that space plays a crucial role in indexing declarative memories. Animal and patient studies (e.g. Chalfonte *et al.*, 1996; Brown and Aggleton, 2001; Eacott and Gaffan, 2005; Piekema *et al.*, 2006; Ranganath, 2010; Libby *et al.*, 2014) documented a functional parcellation of the MTL with separate structures representing respectively the environmental layout, the objects within it, as well as binding the latter to the former. According to this view, space is crucial for recalling events, but not for binding object features. Olson *et al.* (2006) for example, reported that patients with post-anoxic or post-encephalitic MTL pathology had impaired object-location binding in a WM task. This impairment was unaccounted by either diminished recognition or spatial memory. In animals, MTL lesions are also followed by dissociated impairments in object recognition and recall of object-location conjunctions, suggesting that feature and spatial binding depend on distinct MTL processes (Meunier *et al.*, 1993; Murray and Mishkin, 1998; Malkova and Mishkin, 2003). Studies in temporal lobe epilepsy (TLE) patients reported deficits in spatial recall, spatial binding and visual recognition (Abrahams *et al.*, 1997; Bohbot *et al.*, 1998; Stepankova *et al.*, 2004), however it remains unclear whether these impairments should be

attributed to diminished spatial precision (Kolarik *et al.*, 2016) or a binding deficit (Zokaei *et al.*, 2019) and whether binding impairments are dimensionally general (Hannula *et al.*, 2006; Pertzov *et al.*, 2013) or specific.

To examine these issues, we tested TLE patients who had undergone temporal lobectomies and healthy controls with two tasks used in a previous investigation of a stroke patient (Dundon *et al.*, 2017). The first requires recalling the color of one of two polygons identified by either a location or a shape probe, thus directly pitting spatial vs. non-spatial binding. The second probes participants' ability to estimate the average position of three visible disks. In this task healthy participants show a pseudo-neglect pattern of leftward static errors (Baud-Bovy and Soechting, 2001), which suggests that centroid estimation is sensitive to attentional biases (Dundon *et al.*, 2017). The centroid task was therefore used to highlight the presence of unilateral neglect, which can follow lesions of the non-dominant parahippocampal cortex (Mort *et a.l*, 2003) as well as the integrity of spatial perception and attention (Drew *et al.*, 2010).

Material and Methods

The aim of the present study was to compare non-spatial and spatial binding performance in TLE patients' with medically refractory epilepsy who had undergone temporal lobectomy and healthy controls. Recruitment and testing took place at the Neuropsychology section of the Department of Neurosciences of the Department of Neurosciences of King Faisal Specialist Hospital & Research Centre in Riyadh, Saudi Arabia. The experimental protocol was approved by the local Institutional Review Board. Participants gave written informed consent prior to engaging in any experimental procedure.

Study participants

Over a month period, an opportunity sample of patients attending the Neurology and Neurosurgical Clinics were invited to participate in the study. All had been diagnosed with TLE on the basis of clinical presentation and instrumental diagnostic procedures, inclusive of ambulatory EEG and neuroimaging, and after failing medical therapy, had undergone surgical treatment. All patients had normal or corrected to normal visual acuity. Those with an estimated full-scale IQ of less than 75, as assessed with an Arabic version of the Wechsler Abbreviated Scale of Intelligence – Second Edition (WASI-II, Al-Joudi *et al.*, 2019), were excluded, as well as those with a history of traumatic brain injury or major psychiatric disorders. Patients who suffered a seizure in the preceding 48 hours had the testing session postponed. Thirteen patients took part in this study. The study's neurosurgeon identified the anatomical structures involved by the resection on the basis of the surgical record and post-surgical MRI scans.

Fifteen healthy participants were concurrently recruited from the local community as controls. Potential participants were excluded if they had a history of a major neurological or psychiatric disorder or an uncorrected visual impairment or an estimated IQ less than 75.

Testing protocol

Testing took place in a quiet, dimly lit room. Participants sat comfortably at a distance of approximately 70cm from a MacBook Pro® set at a resolution of 1680x1050 pixels. Custom-coded Matlab (Mathworks, Natick, Massachusetts) scripts used a set of freely available routines (Brainard, 1997) to control the timing of the displays. Two tasks were conducted using the computerized set-up.

Cued color recall

In each trial, an equilateral triangle and a square, whose side lengths are 1.29° and 0.92° respectively, appear side-to-side in the lower half of the screen, as shown in figure 1A. The shapes are centred at an eccentricity of 2.27° along the main screen diagonals and remain visible for 2.0s. The two shapes are of different colors, either red, blue or green. The sample display is followed by a 0.2s long pattern mask and a 1.3s blank screen. The recall screen contains three colored rectangles, 0.53° wide and 1.59° high, whose lower edges are aligned 1.39° above the screen center and spaced horizontally 4.81° apart. A bright cross (location probe) or the outline of one of the polygons (shape probe) identifies the target. The location probe, which also includes a dark cross, appear at the locations occupied by the two shapes. The shape cue appears 3.0° below the screen center. Participants report the target color by placing the cursor over the corresponding colored rectangle and clicking the mouse button. The mouse click prompts the beginning of a new trial after a 1.0s delay during which the screen is blank. Participants practiced the task over 16 trials and then completed two blocks of 96 trials each, including both shape and location cued recalls. Trial order was randomised, minimizing participants' ability to predict whether a shape or location probe

would follow the sample display. To ensure that patients had not forgotten the task instructions, at the end of each block they were asked to describe what they had done.

Centroid estimation

This task assesses the accuracy and precision of estimates of the average location of three visible white disks and is illustrated in figure 1B. Each disk's diameter is 0.27°. Participants place a crosshair-shaped cursor at the estimated centroid location and click the mouse. Following a 1.0s interval, a novel set of disks appears and the procedure is repeated. Disks can occupy any three of seven canonical locations, including the screen center and the vertices of a virtual concentric hexagon, with a side length of 3.67°. All permutations of three canonical locations, less any resulting in a collinear configuration, are used as test arrays. Each possible permutation appears twice, for a total of 64 trials. Pseudorandom, zero mean, independent circular Gaussian distributions, with a standard deviation of 0.6°, are sampled to jitter each disk's position. Prior to testing, instructions were read to the participants. The centroid was defined as the point where the triangle, whose vertices coincided with the disks' locations, would balance in the horizontal plane (Baud-Bovy and Soechting, 2001). Participants completed 25 practice trials, without feed-back, followed by two blocks of 64 trials each.

Neuropsychological tests

Three neuropsychological instruments were used to assess participants: 1) Hopkins Verbal Learning Test – Revised (HVLT-R), 2) Brief Visuospatial Memory Test – Revised (BVMT-R), and 3) Color Trails Test (CTT). The Arabic version of these tests were recently validated (Al-Joudi *et al.*, 2019).

Data analysis

In the recall task, participants could either report 1) the color of the target, correct response, 2) the color of the non-target item, that is make a swap error, or 3) the color absent from the sample, that is make a generic error. We approached the group level hypothesis testing as a metanalysis of prevalence data, treating each participant as a separate study. All inferential analysis presented in this study is Bayesian.

Group differences in recall error rates

Group level effects were analysed with mixed Bayesian ANOVAs using the JASP software (JASP Team, 2021; jasp-stats.org). The between group variable coded whether the participant was 1) a healthy control, 2) a patient following left or 3) right temporal lobectomy, respectively. The within group variables were probe dimension, i.e., whether a shape or space probe was used to cue recall, and block order, i.e., first or second block. The error rates were normalised with a Friedman-Tukey double arcsine transformation (Barendregt et al., 2013). The transformation stabilizes error rates variances and allows the use of parametric methods to compute group statistics:

$$\boldsymbol{t} = \sin^{-1}\sqrt{\frac{\boldsymbol{c}}{n}} + \sin^{-1}\sqrt{\frac{\boldsymbol{c}}{n+1}}$$

where $\boldsymbol{c}$ is the number of either swap or generic errors and n is the total number of trials for each probe dimension and block. The group average proportions were obtained by applying the following inverse transformation to the transformed proportions group means:

$$\hat{p} = \left[1 - sgn(\cos\hat{t}) \cdot \sqrt{1 - \left(\sin\hat{t} - \frac{\sin\hat{t} - 1/\sin\hat{t}}{n}\right)^2}\right] \cdot 0.5$$

Analysis of centroid task

The analysis of the centroid task was carried out by fitting the following regression model to each participants' reports:

$$\begin{pmatrix} \boldsymbol{r}_x \\ \boldsymbol{r}_y \end{pmatrix} = \begin{pmatrix} a_0 \\ b_0 \end{pmatrix} + \begin{pmatrix} a_1 & 0 \\ 0 & b_1 \end{pmatrix} \begin{pmatrix} \boldsymbol{C_x} \\ \boldsymbol{C_y} \end{pmatrix} + \begin{pmatrix} \boldsymbol{N}_x \\ \boldsymbol{N}_y \end{pmatrix}$$

where $\boldsymbol{r}_x$ and $\boldsymbol{r}_y$ are the *x*-*y* screen coordinates of the centroid estimates, $\boldsymbol{C}_x$, $\boldsymbol{C}_y$ are the centroid horizontal and vertical screen coordinates and $\boldsymbol{N}_x$ and $\boldsymbol{N}_y$ are the normal distributions of the respective residuals. Although incenter biases are also known to affect centroid estimates (Baud-Bovy and Soechting, 2001), we did not include them in the model for sake of clarity and because a preliminary analysis did not reveal appreciable group differences. Group and screen coordinates differences in static offsets, i.e. a_0 and b_0, accuracy, i.e. a_1 and b_1, and precision, i.e. the variance of $\boldsymbol{N}_x$ and $\boldsymbol{N}_y$, were assessed with Bayesian mixed ANOVAs.

Results

Participants' demographic, clinical and neuropsychometric characteristics

Table 1 reports the demographic and clinical characteristics of the left and right temporal lobectomy patients and healthy controls. The groups were matched on age, gender and educational level. Both patient groups showed a lower full-scale IQ that healthy controls, however all of the variables were more likely to reflect a null effect than a group difference. Table 2 details the sex, education level and neuropsychometric performance of the thirteen patients. Both raw scores as well the values normalised on the basis of a reference sample of healthy controls, whose first language is Arabic (Al-Joudi *et al.*, 2019), are shown. We examined whether patients showed a material specific pattern of lateralized deficits (e.g. Saling, 2009) by comparing performance of the left and right temporal lobectomy patients on the HMVT and the BVMT with Bayesian independent samples t-tests (JASP Team, 2021; jasp-stats.org). There was moderate strength evidence for left temporal lobectomy patients having worse delayed verbal recall on the HVLT than controls (BF_{10} = 7.99), while there was anecdotal evidence for no group difference in the delayed visuo-spatial recall (BF_{10} = 0.46). In Table 3 the MTL structures affected by the surgical excisions are listed, patient by patient, while Table 3-1 (see supplementary material) shows representative postsurgical axial, sagittal and coronal multimodal MRI slices for each patient.

Cued color recall performance

In the cued recall task, participants completed two blocks of 96 trials each. Mixed effect Bayesian ANOVAs were used to examine the influence of three factors on recall: 1) group, namely whether participants were controls, patients following left and right temporal lobectomy, respectively; 2) block and 3) probe dimension. Generic and swap errors were analysed separately.

Extended data table 4-1 reports the result of the ANOVA model comparison for swap errors. The model with the highest posterior probability included group, probe dimension and block, as well as the interaction of group by probe dimension. Table 4 summarises the evidence for each predictor. There was moderate evidence for an effect of probe dimension and block. There was very strong evidence for an effect of group and strong evidence for an interaction of group by probe dimension.

Extended data table 5-1 summarises the results of the model comparisons for generic errors. The best model was the one which included all three factors, but none of the interactions. Table 5 summarises the analysis of the effects. There was anecdotal evidence for the block and probe dimension affecting the proportion of generic errors. On the other hand, there was anecdotal evidence for a null effect of group.

Figure 2 shows the mean proportion of swap and generic errors following space and shape probe, respectively. Controls made fewest swap and generic errors. Controls and patients with right temporal lobectomies made more swap errors following shape than space probes. Patients with left temporal lobectomies made most swap errors and three of them made more swap errors following space than shape probes. Participants made more generic errors following space than shape probe. Participants also made more swap and generic errors in the first than second block (data not shown).

Centroid estimation performance

We examined how group and screen coordinates affected three indices of performance in the centroid estimation task: 1) static offsets, 2) accuracy and 3) precision (see Methods). For static offsets the model with the highest posterior probability included the effect of screen coordinates only. In fact, there was strong evidence, $BF_{inc} = 32.13$, that the horizontal and vertical offsets differed. While there was no appreciable horizontal bias, $m = 0.0°$, *95%CI* =

[-0.04°, 0.05°], participants showed an upward bias, m = 0.15°, *95%CI* = [0.07°, 0.23°]. There was moderate evidence in favour of the null and against both an effect of group, BF_{inc} = .22, and its interaction with coordinate, BF_{inc} = .28. For accuracy, the model with highest posterior probability included group. However, there was anecdotal evidence for a null effect of group, BF_{inc} = .76, with moderate evidence in favour of a null effect of coordinate (BF_{inc} = .26), and its interaction with group, BF_{inc} = .28. For precision, namely the variance of the variable errors, the null model had the highest posterior probability. There was anecdotal evidence for a null effect of screen coordinate, BF_{inc} = 0.4, anecdotal evidence for a null effect of group, BF_{inc} = 0.53, and moderate evidence for a null interaction of group and dimension, BF_{inc} = 0.15.

Discussion

In this study we compared performance of healthy controls and temporal lobectomy patients in two tasks, one probing conjunctive binding in vWM, the other perceptual, spatial averaging of disks patterns. The vWM task required the recall of a target's colour, where the target was identified by either a location or a shape probe. The task was thus designed to determine dimensional specificity of working memory conjunctive binding. Controls were more accurate than patients overall. Moreover, they made fewer swap errors following space than shape probes, while left temporal lobectomy patients made more swap errors following space than shape probes. There was no evidence of group differences in static biases, accuracy and precision of perceptual centroid estimates. The implication of these findings for the organization of binding and spatial processes in vWM is discussed in the next paragraph, following a brief overview of prior evidence.

MTL lesions specifically disrupt spatial binding in vWM

Previous studies addressed whether MTL pathology is associated with impairments in vWM binding. The ability to recall shape-color, shape-location or item-item conjunctions has been found to be diminished in patients with anoxic/ischemic or infectious pathology involving the MTL as well as neurodegenerative disorders, suggesting an impairment in conjunctive and relational binding (Hannula *et al*., 2006; Olson *et al*., 2006; Parra *et al*., 2009). van Geldorp, Bouman, Hendriks and Kessels (2014) compared patients, who had undergone anterior temporal lobectomies for medically refractory epilepsy, and healthy controls' performance in four match-to-sample tasks. The tasks were difficult and required participants to remember three separate frames presented sequentially. Each frame contained the picture of a face and a building, which differed in location and color. A cue, presented before the sample indicated whether participants should only remember the identity of the

items or also their location (spatial binding condition), color (color binding condition) or the item they had been presented with (relational binding condition). Overall, recall was less accurate in patients compared to controls, and particularly so in the relational binding condition. Recall performance in the spatial and color binding conditions were equally affected, suggesting that spatial and non-spatial WM binding were not differentially compromised in these patients. Zokaei *et al*. (2019) found that patients, who had undergone a temporal lobectomy, made more swap errors when recalling the location of fractal patterns, compared to controls. Since neither fractal recognition nor memory for locations were found to be appreciably impaired in these patients, it was inferred that they suffered a primary binding deficit. Using a similar paradigm, Pertzov *et al.* (2013) documented both a spatial as well as a non-spatial binding deficit in individuals recovering from autoimmune encephalitis, suggesting that binding impairments due to MTL dysfunction are not dimensionally specific. Braun *et al.* (2011) concluded instead that TLE patients, who had undergone a right temporal lobectomy, were only impaired when the vWM task required spatial binding, but performed similarly to healthy controls when it required binding of non-spatial features.

Our own findings contribute new, crucial evidence for understanding the role of MTL in vWM binding by confirming the association between MTL pathology and spatial binding impairments, unaccounted for by impairments of either spatial vision or feature memory. We found an increase in the proportion of swap errors in the TLE group. Crucially, while healthy participants made significantly more swap errors following the shape probe, left temporal lobectomy patients made more swap errors following the space probe. In healthy participants the results are therefore in keeping with the hypothesis that binding of non-spatial features is mediated by the features' shared location (e.g., Schneegans and Bays, 2017; Treisman and Zhang, 2006). In fact, the likelihood of swap errors should be greater following shape compared to space probes, because in the latter case both target shape and color need to be

bound to the target location before they can be bound to each other (Schneegans and Bays, 2017). On the other hand, the observation that some patients made significantly more swap errors following space probes than controls may indicate that patients gained the ability to bind non-spatial features directly, without the mediation of a shared location, allowing them to achieve higher accuracies following shape than space probes. Whether this inference is warranted remains to be established. Regardless, the group level pattern of dimensionally specific binding impairments observed in left TLE patients replicates a previous observation in a stroke patient with bilateral MTL damage, found to be impaired only in vWM tasks requiring spatial binding, but not those requiring non-spatial binding (Dundon *et al.*, 2017). These observations thus allow us to draw the following conclusion: MTL pathology can be associated with WM binding impairments that are spatially specific and reverse the spatial advantage characteristic of healthy controls. If processes underlying spatial binding in vWM are independent from processes devoted to binding of non-spatial features, then the role of space in organising vWM may extend beyond providing a common index for the conjunctive binding of visual features.

Hemispheric lateralization and binding

Bohbot *et al.* (1998) found that patients who had undergone thermocoagulation of structures within the right, but not the left MTL were more impaired in a number of spatial WM tasks than those who had not undergone surgery, suggesting that right MTL structures may play an overarching role in spatial memory. Braun *et al.* (2011) compared patients with right temporal lobectomy and healthy controls' performance on a number of single feature and feature conjunction recall tasks and concluded that these patients are specifically impaired in spatial binding. However, the tasks employed memory samples of different complexity to probe recall of features and conjunctions, respectively, thus introducing a load

confound in the comparison. Our own results are in keeping with the idea that left rather than right MTL structures are specifically involved in spatial binding, since patients who had undergone left temporal lobectomies showed greater spatial binding impairments than patients with right temporal lobectomies. While our results need to be interpreted cautiously, given the small sample size, they agree with the conclusion drawn by Kessels *et al.* (2004), who found that patients who had undergone left, but not right temporal lobectomies were impaired in spatial binding, confirming lateralization effects previously observed by the same group in a sample of patients with cerebrovascular pathology (Kessels *et al.*, 2002). Spiers *et al.* (2001) found that left temporal lesion specifically affect object location binding while right temporal lesions affect spatial memory more generally. However, the existing literature remains inconclusive to the relation between laterality and working memory spatial binding. A distinct view of lateralization of binding impairments is that the latter reflect attention deficits which follow cortical strokes, especially involving the non-dominant right hemisphere. For example. Cohen-Dallal *et al.* (2021) reported that patients with unilateral attentional neglect show delay-dependent decrements in spatial binding performance. In light of the fact that parahippocampal damage is associated with unilateral neglect (Mort *et al.*, 2003), Cohen-Dallal *et al.*'s finding raises the possibility that lateralized attentional deficits may also contribute to the binding impairments observed in our study. However, performance in a centroid estimation task did not show group differences in lateralized static biases, suggesting that lesion in our sample was not associated with unilateral neglect. Moreover, patients showed neither diminished accuracy nor lower precision in the centroid task compared to controls, indicating that spatial perception and attention were not compromised (Drew *et al.*, 2010).

A further concern is that uncontrolled verbal strategies may have confounded the interaction of lesion laterality and probe dimension. We found in pilot studies that healthy

participants maintain a spatial advantage in WM binding under condition of articulatory suppression and therefore concluded that the spatial advantage in WM binding does not depend on verbal strategies (unpublished data). However, we cannot rule out the possibility that left temporal lobectomy patients used a verbal strategy and thus managed to selectively improve binding of shape and color.

It is important to note, with regard to the issue of localization and the nature of cognitive impairments encountered in TLE patients, that group level results belie substantial inter-individual differences (see Figure 2). Previous electrophysiological recordings from the left MTL indicated that trial by trial changes in the amplitude of low-frequency oscillations, obtained during encoding episodes, predict subsequent recall accuracy of object/place conjunctions in TLE patients (Miller et al., 2018), in keeping with our own conclusion that spatial binding is dependent on left lateralized processes. Interestingly, this was not the case in all suggesting that spatial binding processes are not universally left lateralised in these patients. Unfortunately, the study did not report whether the lateralization of spatial binding processes was affected by the laterality of the seizure focus, precluding firmer conclusion regarding the relation between the two. Other studies have, however, demonstrated anomalous lateralization in high proportion of TLE patients, as memory processes often shift to the contra-lesional hemisphere both pre (Bellgowan *et al.*,1998; Golby *et al.*, 2002; Janszky *et al.*, 2004) and postoperatively (Sidhu *et al.*, 2016). These findings may provide one possible interpretation of the interindividual differences highlighted above, namely that neural plasticity in some TLE patients modifies the lateralization of memory processes usually encountered in healthy controls. An alternative explanation, initially born out of observations in non-human primates with focal lesions (Browning *et al.*, 2010; Croxson et al., 2012), is that effects of MTL functional and structural damage in postsurgical TLE patients may be attenuated by non-lateralized recruitment of neocortical areas (Sidhu *et al.*, 2013). To

415 determine whether either or both of these hypotheses can account for interindividual
416 differences in spatial binding impairments and to what extent other factors, like age of seizure
417 onset, severity and frequency of seizures, neuropsychiatric complications and antiepileptic
418 medications, known to affect neural plasticity and degree of cognitive impairment (Bell *et al.*,
419 2011), also contribute to hemispheric lateralization in TLE patients will require new
420 experimental evidence.

421 Despite the potential confound listed above, the present study indicates that following
422 left temporal lobectomy, vWM binding is diminished in a dimensionally specific manner in
423 the absence of appreciable perceptual, attentional or visual-spatial memory deficits.

References

Abrahams S, Pickering A, Polkey CE, Morris RG (1997) Spatial memory deficits in patients with unilateral damage to the right hippocampal formation. *Neuropsychologia* 35: 11-24.

Al-Joudi HF, Mincari L, Baz S, Nester M, Al-Marzouki N, Abalkhail T, Aljehani N, et al. (2019) Standardization of an Arabic-Language Neuropsychological Battery for Epilepsy Surgical Evaluations. *J Int Neuropsych Soc* 25: 761-71.

Allen RJ, Vargha-Khadem F, Baddeley AD (2014) Item-location binding in working memory: Is it hippocampus-dependent? *Neuropsychologia* 59: 74-84.

Alvarez GA, Cavanagh, P (2004) The capacity of visual short-term memory is set both by visual information load and by number of objects. *Psychol Sci* 15: 106-111.

Baddeley AD, Allen RJ, Hitch GJ (2011) Binding in visual working memory: the role of the episodic buffer. *Neuropsychologia* 49: 1393-400.

Barendregt, J. J., Doi, S. A., Lee, Y. Y., Norman, R. E., Vos, T (2013) Meta-analysis of prevalence. *J Epidemiol Community Health* 67: 974-8.

Baud-Bovy G, Soechting J (2001) Visual localization of the center of mass of compact, asymmetric, two-dimensional shapes. *J Exp Psychol Hum Percept Perform* 27: 692-706.

Bays PM, Catalao RFG, Husain M (2009) The precision of visual working memory is set by allocation of a shared resource. *J Vision* 9: 7.

Bays PM, Wu EY, Husain M (2011) Storage and binding of object features in visual working memory. *Neuropsychologia* 49: 1622-31.

Bell B, Lin JJ, Seidenberg M, Hermann B (2011) The neurobiology of cognitive disorders in temporal lobe epilepsy. *Nat Rev Neurol* 7: 154-64.

447 Bellgowan PSF, Binder JR, Swanson SJ, Hammeke TA, Springer JA, Frost JA, Morris
448 GL (1998) Side of seizure focus predicts left medial temporal lobe activation during verbal
449 encoding. *Neurology* 51: 479-84.
450 Bohbot VD, Kalina M, Stepankova K, Spackova N, Petrides M, & Nadel L (1998)
451 Spatial memory deficits in patients with lesions to the right hippocampus and to the right
452 parahippocampal cortex. *Neuropsychologia* 36: 1217-38.
453 Brainard DH (1997) The Psychophysics Toolbox. *Spat Vis* 10: 433-6.
454 Braun M, Weinrich C, Finke C, Ostendorf F, Lehmann TN, Ploner CJ (2011) Lesions
455 affecting the right hippocampal formation differentially impair short-term memory of spatial
456 and nonspatial associations. *Hippocampus* 21: 309-18.
457 Brown M, Aggleton J (2001) Recognition memory: what are the roles of the perirhinal
458 cortex and hippocampus? *Nat Rev Neurosci* 2: 51-61.
459 Browning PG, Gaffan D, Croxson PL, Baxter MG (2010) Severe scene learning
460 impairment, but intact recognition memory, after cholinergic depletion of inferotemporal
461 cortex followed by fornix transection. *Cereb Cortex* 20: 282-93.
462 Carlesimo GA, Perri R, Turriziani P, Tomaiuolo F, Caltagirone C (2001) Remembering
463 what but not where: independence of spatial and visual working memory in the human
464 brain. *Cortex* 37: 519-34.
465 Chalfonte BL, Verfaellie M, Johnson MK, Reiss L (1996) Spatial location memory in
466 amnesia: binding item and location information under incidental and intentional encoding
467 conditions. *Memory* 4: 591-614.
468 Cohen-Dallal H, Soroker N, Pertzov Y (2021) Working Memory in Unilateral Spatial
469 Neglect: Evidence for Impaired Binding of Object Identity and Object Location. *J Cogn*
470 *Neurosci* 33: 46-62.

471 Drachman DA, Arbit J (1966) Memory and the hippocampal complex: II. Is memory a
472 multiple process? *Arch Neurol* 15: 52-61.
473 Drew SA, Chubb CF, Sperling G (2010) Precise attention filters for Weber contrast
474 derived from centroid estimations. *J Vision* 10: 20-20.
475 Dundon NM, Katshu MZUH, Harry B, Roberts, D, Leek EC, Downing P, Sapir A,
476 d'Avossa (2017) Human parahippocampal cortex supports spatial binding in visual working
477 memory. *Cereb Cortex* 28: 3589-99.
478 Eacott MJ, Gaffan EA (2005) The roles of perirhinal cortex, postrhinal cortex, and the
479 fornix in memory for objects, contexts, and events in the rat. *Q J Exp Psychol B* 58: 202–17.
480 Finke C, Braun M, Ostendorf F, Lehmann TN, Hoffmann KT, Kopp U (2008) The
481 human hippocampal formation mediates short-term memory of color–location
482 associations. *Neuropsychologia* 46: 614-623.
483 Golby AJ, Poldrack RA, Illes J, Chen D, Desmond JE, Gabrieli, J D (2002) Memory
484 lateralization in medial temporal lobe epilepsy assessed by functional MRI. *Epilepsia* 43:
485 855-63.
486 Hannula DE, Tranel D, Cohen NJ (2006) The long and the short of it: relational memory
487 impairments in amnesia, even at short lags. *J Neurosci* 26: 8352-9.
488 Holdstock JS, Shaw C, Aggleton JP (1995) The performance of amnesic subjects on tests
489 of delayed matching-to-sample and delayed matching-to-position. *Neuropsychologia* 33:
490 1583-96.
491 Janszky J, Ollech I, Jokeit H, Kontopoulou K, Mertens M, Pohlmann-Eden B,
492 Woermann, FG. (2004) Epileptic activity influences the lateralization of mesiotemporal fMRI
493 activity. *Neurology* 63: 1813-7.
494 JASP Team (2021). JASP (Version 0.15.0.0) [Computer software]. https://jasp-stats.org/.

Jeneson A, Mauldin KN, Squire LR (2010) Intact working memory for relational information after medial temporal lobe damage. *J Neurosci* 30: 13624-9.

Kessels RP, Kappelle LJ, de Haan EH, Postma A (2002) Lateralization of spatial-memory processes: evidence on spatial span, maze learning, and memory for object locations. *Neuropsychologia* 40: 1465-73.

Kessels RP, Hendriks MP, Schouten J, Van Asselen M, Postma A (2004) Spatial memory deficits in patients after unilateral selective amygdalohippocampectomy. *J Int Neuropsych Soc* 10: 907-12.

Kolarik BS, Shahlaie K, Hassan A, Borders AA, Kaufman KC, Gurkoff G (2016) Impairments in precision, rather than spatial strategy, characterize performance on the virtual Morris Water Maze: A case study. *Neuropsychologia* 80: 90-101.

Libby LA, Hannula DE, Ranganath C (2014) Medial temporal lobe coding of item and spatial information during relational binding in working memory. *J Neurosci* 34: 14233-42.

Luck SJ, Vogel EK (1997) The capacity of visual working memory for features and conjunctions. *Nature* 390: 279-81.

Luck SJ, Vogel EK (2013) Visual working memory capacity: from psychophysics and neurobiology to individual differences. *Trends Cogn Sci* 17: 391-400.

Malkova L, Mishkin M (2003) One-trial memory for object-place associations after separate lesions of hippocampus and posterior parahippocampal region in the monkey. *J Neurosci* 23: 1956-65.

Meunier M, Bachevalier J, Mishkin M, Murray EA (1993) Effects on visual recognition of combined and separate ablations of the entorhinal and perirhinal cortex in rhesus monkeys. *J Neurosci* 13: 5418-32.

518 Miller J, Watrous AJ, Tsitsiklis M, Lee SA, Sheth SA, Schevon CA, Jacobs J. (2018)
519 Lateralized hippocampal oscillations underlie distinct aspects of human spatial memory and
520 navigation. *Nat Commun* 9: 1-12.
521 Mort DJ, Malhotra P, Mannan SK, Rorden C, Pambakian A, Kennard C, & Husain M.
522 (2003) The anatomy of visual neglect. *Brain* 126: 1986-97.
523 Murray EA, Mishkin M (1998) Object recognition and location memory in monkeys
524 with excitotoxic lesions of the amygdala and hippocampus. *J Neurosci* 18: 6568-82.
525 Olson IR, Page K, Moore KS, Chatterjee A, Verfaellie M (2006) Working memory for
526 conjunctions relies on the medial temporal lobe. *J Neurosci* 26: 4596-601.
527 Olton DS, Becker JT, Handelmann GE (1979) Hippocampus, space, and memory. *Behav*
528 *Brain Sci* 2: 313–65.
529 Parra MA, Abrahams S, Fabi K, Logie R, Luzzi S, Sala SD (2009) Short-term memory
530 binding deficits in Alzheimer's disease. *Brain* 132: 1057-66.
531 Pertzov Y, Miller TD, Gorgoraptis N, Caine D, Schott JM, Butler C (2013) Binding
532 deficits in memory following medial temporal lobe damage in patients with voltage-gated
533 potassium channel complex antibody-associated limbic encephalitis. *Brain* 136: 2474-85.
534 Piekema C, Kessels RP, Mars RB, Petersson KM, Fernández G (2006) The right
535 hippocampus participates in short-term memory maintenance of object–location
536 associations. *Neuroimage* 33: 374-82.
537 Ploner CJ, Gaymard BM, Rivaud-Péchoux S, Baulac M, Clémenceau S, Samson S
538 (2006) Lesions affecting the parahippocampal cortex yield spatial memory deficits in
539 humans. *Cereb Cortex* 10: 1211-6.
540 Ranganath C (2010) A unified framework for the functional organization of the medial
541 temporal lobes and the phenomenology of episodic memory. *Hippocampus* 20: 1263-90.

542 Saling MM (2009) Verbal memory in mesial temporal lobe epilepsy: beyond material
543 specificity. *Brain* 132: 570-82.
544 Salvatier J, Wiecki TV, Fonnesbeck C (2016) Probabilistic programming in Python
545 using PyMC3. *PeerJ Computer Science* 2, e55.
546 Schneegans S, Bays PM (2017) Neural architecture for feature binding in visual working
547 memory. *J Neurosci* 37: 3913-25.
548 Sidhu MK, Stretton J, Winston GP, Bonelli S, Centeno M, Vollmar C, Symms M,
549 Thompson PJ, Koepp MJ, Duncan J (2013) A functional magnetic resonance imaging study
550 mapping the episodic memory encoding network in temporal lobe epilepsy. *Brain* 136: 1868-
551 88.
552 Sidhu MK, Stretton J, Winston GP, McEvoy AW, Symms M, Thompson PJ, Koepp MJ,
553 Duncan JS (2016) Memory network plasticity after temporal lobe resection: a longitudinal
554 functional imaging study. *Brain* 139: 415-30.
555 Smyrnis N, d'Avossa G, Theleritis C, Mantas A, Ozcan A, Evdokimidis I (2005) Parallel
556 processing of spatial and serial order information before moving to a remembered target. *J*
557 *Neurophysiol* 93: 3703-8.
558 Sokal RR, Rohlf FJ (1995) Biometry. New York: W. H. *H. Freeman and Company*.
559 Squire LR (2009) The legacy of patient H.M. for neuroscience. *Neuron* 61: 6-9.
560 Spiers HJ, Burgess N, Maguire EA, Baxendale SA, Hartley T, Thompson PJ, O'Keefe J
561 (2001) Unilateral temporal lobectomy patients show lateralized topographical and episodic
562 memory deficits in a virtual town. *Brain* 124: 2476-89.
563 Stepankova K, Fenton AA, Pastalkova E, Kalina M, Bohbot VD (2004) Object-location
564 memory impairment in patients with thermal lesions to the right or left hippocampus.
565 *Neuropsychologia* 42: 1017-28.

Treisman A, Zhang W (2006) Location and binding in visual working memory. *Mem Cogn* 34: 1704-19.

van Geldorp B, Bouman Z, Hendriks MP, Kessels RP (2014) Different types of working memory binding in epilepsy patients with unilateral anterior temporal lobectomy. *Brain Cogn* 85: 231-8.

Vehtari A, Gelman A, Sivula T, Jylänki P, Tran D, Sahai S, Robert CP (2020) Expectation Propagation as a Way of Life: A Framework for Bayesian Inference on Partitioned Data. *Journal of Machine Learning Research* 21: 1-53.

Zhang W, Luck SJ (2008) Discrete fixed-resolution representations in visual working memory. *Nature* 453: 233-5.

Zokaei N, Nour MM, Sillence A, Drew D, Adcock J, Stacey R (2019) Binding deficits in visual short-term memory in patients with temporal lobe lobectomy. *Hippocampus* 29: 63-7.

Legends

Figure 1. Tasks' structure. Panel A shows the event sequence in the color recall task. Participants had to remember the color of a triangle and a square displayed side by side. The sample display was followed by a pattern mask and a blank screen. The recall target was identified either by a space probe, consisting a bright cross displayed at the location. previously occupied by the target, or by a shape probe, consisting of the outline of the target shape. The color was reported by placing the cursor over the corresponding rectangle and clicking the mouse button. Panel B shows the centroid estimation task. The visual display contained 3 bright dots and the participant had to indicate the location of the center of mass of the imaginary triangle whose vertices corresponded to the dots location, by dragging the cursor and clicking.

Figure 2. Recall error rates. The bar graph on the left shows the group averaged proportions of swap errors, while the bar graph on the right shows the group averaged proportions of generic errors, following space and shape probes, respectively. Overall patients made more swap errors than controls. Moreover, patients with left temporal lobectomies made more swap errors following space than shape probes, suggesting a specific impairment of spatial binding in this group only. For generic errors, group differences were marginal and were not further affected by probe dimension. For sake of clarity, the data are averaged over the two blocks. Circles are individual participants' error rates. Continuous lines join swap error rates, following space and shape probes respectively, of each left temporal lobectomy patient. Broken lines join the swap error rates of each right temporal lobectomy patient. Error bars are standard errors of the mean.

603 **Table 1. Demographic and clinical sample characteristics.** Group frequencies were
604 compared using a Bayesian contingency table. Continuous variables were compared with
605 Bayesian ANOVAs or Bayesian independent samples t-test. The values in parenthesis are
606 standard deviations. None of the demographic or clinical variables showed appreciable group
607 differences since the Bayes factor (BF_{10}) was less than 1.0 for all comparisons.
608
609 **Table 2. Demographics and neuro-psychometric performance of TLE patients.** Raw
610 scores are reported for each test and participant (see methods). The corresponding normalised
611 values are shown in parenthesis. Normalised z-scores values were computed by subtracting
612 the mean score and dividing by the standard deviation of a reference sample (Al-Joudi et al.,
613 2019). To facilitate inspection of the table scores corresponding to better than mean
614 performance are underlined. HVLT-R = Hopkins Learning Test – Revised; BVMT-R = Brief
615 Visuospatial Memory Test – Revised; CTT = Colour Trails Test.
616
617 **Table 3. Patients' lesion anatomy.** The table lists the pathology and regions affected by the
618 lobectomy for each patient. Table 3-1 of the extended data shows representative MRI slices
619 through the medial temporal lobes. GG, ganglioglioma; MG, meningioma; MTS, medial
620 temporal sclerosis; HIP, hippocampus; ERC, entorhinal cortex; PRC, perirhinal cortex; PHC,
621 parahippocampal cortex; ITC, inferotemporal cortex; MTG, Middle temporal gyrus; ATP,
622 anterior temporal pole; STG, superior temporal gyrus; AMG, amygdala. ''0'' indicates an
623 unaffected subregion, ''+'' a rostro-caudal lesion extent up to 20 mm, and ''++'' up to 40
624 mm.
625
626 **Table 3-1 (Extended data). Post-surgical MRI scans for thirteen patients.** The images
627 were obtained with T1 weighted, T2 weighted, Fluid-attenuated Inversion Recovery and

Gradient Recalled Echo sequences. Legend: ERC, Entorhinal Cortex; PHC, Parahippocampal Cortex; PRC, Perirhinal Cortex; Hipp, Hippocampus; AMG, Amygdala; Temporal pole, TP; antSTG, anterior Superior Temporal Gyrus; antMTG, anterior Middle Temporal Gyrus.

Table 4. Swap errors – analysis of effects. The table lists each factor and interaction for swap error rates. Table 4-1 of the extended data lists the models and associated prior and posterior probabilities from which the values in the present table are computed. P(incl) is the prior probability of the effect; P(incl|d) is the posterior probability of the effect; BF_{incl} is Bayes factor. A BF greater than 1.0 favours the effect, a BF less than 1.0 favours a null instead. Values of the BF greater than 3.0 are in bold, to highlight those effects that have at least moderate evidence in their favour. Block, probe dimension, group and the interaction of group by probe dimension all have at least moderately strong evidence in their favour.

Table 4-1 (Extended data). Best model comparisons for swap errors. The table presents each of the model comparisons from the Bayesian ANOVA. The within factors are block (B) and probe dimension (D). The between factor is group G. P(M) is the a-priori model probability, P(M|d) is the posterior model probability. BF_M is the Bayes factor of the model, BF_{10} is the Bayes factor of the model relative to the best one. The best model contained all three factors and the interaction of group by probe dimension.

Table 5. Generic error – analysis of effects. The table lists each factor and interaction for generic error rates. Table 5-1 of the extended data lists the models and associated probabilities, used to compute the effects. P(incl) is the prior probability of the effects; P(incl|d) is the posterior probability of the effect; BF_{incl} is Bayes factor. A BF greater than 1.0

favours the effect, a BF less than 1.0 favours a null effect instead. The only predictors with favourable evidence, albeit of very modest entity, are block and probe dimension.

Table 5-1 (Extended data). Best model comparisons for generic errors. The table presents the model comparisons obtained from a Bayesian ANOVA. The within factors are block (B) and probe dimension (D). The between factor is group G. P(M) is the a-priori model probability, P(M|d) is the posterior model probability. BF_M is the Bayes factor of the model, BF_{10} is the Bayes factor of the model relative to the best one. The best model included the three main factors, namely block (B), probe dimension (D) and group (G).

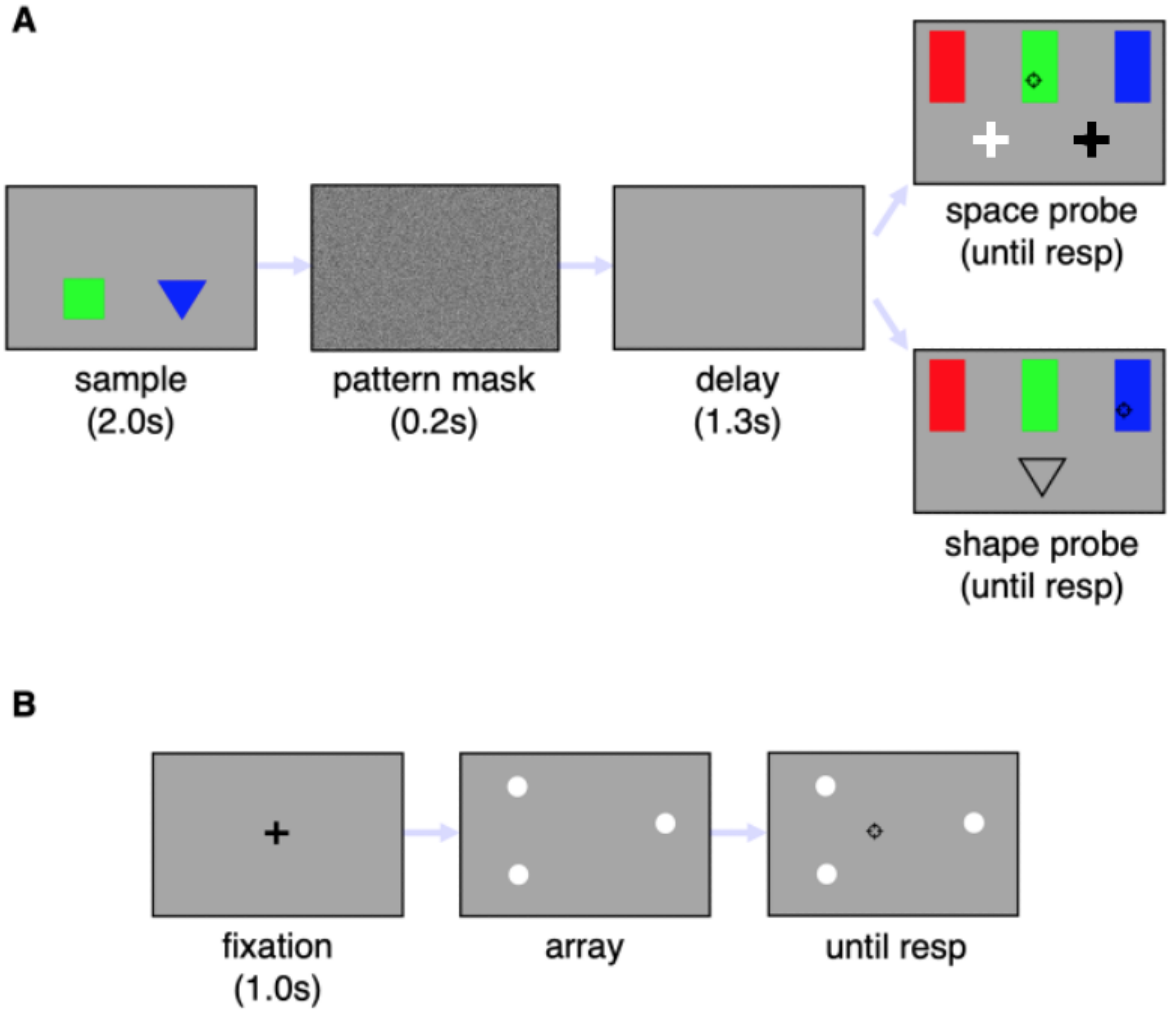

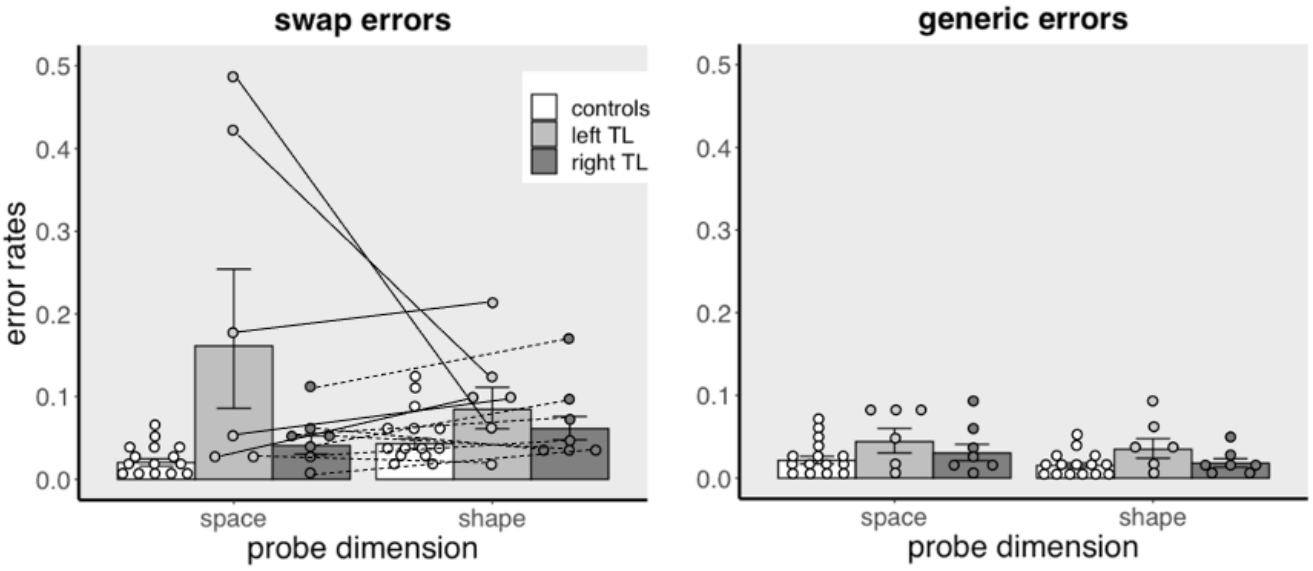

Table 1. Demographic and clinical sample characteristics.

	left TLE (n=6)	right TLE (n=7)	controls (n=15)	BF_{10}
Sex (%males)	83.3	100	93.3	.64
Age (years)	35.2 *(±7.9)*	33.08 *(±8.9)*	33.3 *(±7.8)*	.29
Education (highest grade)	15.3 *(±1.6)*	14.3 *(±1.9)*	14.3 *(±2.4)*	.5
Full Scale IQ	92.0 *(±11.7)*	87.3 *(±9.9)*	99.5 *(±15.5)*	.9
Epilepsy onset age (years)	11.1 *(±10.2)*	22.1 *(±17.2)*	—	.84

Frequency group differences were compared using a Bayesian contingency table. Continuous variables were compared with Bayesian ANOVAs or Bayesian independent samples t-test. The values in parenthesis are standard deviations. None of the demographic or clinical variables showed appreciable group differences since the Bayes factor (BF_{10}) was *less than 1.0 for all comparisons.*

Table 2. Demographics and neuro-psychometric performance of TLE patients

Patient	***Gender***	***Education (years)***	***WAIS II***				***HVLT***			***BVMT***			***CTT***	
			Block Design	*Vocab*	*Matrix Reasoning*	*Similar*	*Immediate*	*Delayed*	*Discrimin*	*Immediate*	*Delayed*	*Discrimin.*	*CTT1 (sec)*	*CTT2 (sec)*
P1	M	16	16 *(-.59)*	18 *(-1.6)*	12*(-.41)*	24 *(-.77)*	19 *(-1.43)*	6 *(-1.47)*	9 *(-1.9)*	12 *(-1.01)*	4*(-1.22)*	4 *(-1.4)*	85 *(1.24)*	160 *(2.0)*
P2	M	14	18 *(-.46)*	27 *(-.83)*	12 *(-.41)*	23 *(-.88)*	26 *(.36)*	9 *(.11)*	12 *(1.1)*	10 *(-1.28)*	4 *(-1.22)*	4 *(-1.4)*	97 *(1.74)*	166 *(2.22)*
P3	F	16	12 *(-.88)*	25 *(-1.0)*	18 *(.53)*	28 *(-.31)*	24 *(-.15)*	7 *(-.95)*	10 *(-.9)*	9 *(-1.41)*	*6 (-.58)*	5 *(-.4)*	65 *(.41)*	130 *(.92)*
P4	M	14	16 *(-.59)*	26 *(-.91)*	14 *(-.09)*	26 *(-.54)*	22 *(-.67)*	7 *(-.95)*	11 *(.1)*	14 *(-.75)*	5 *(-.9)*	4 *(-1.4)*	66 *(.45)*	191 *(3.12)*
P5	M	12	14 *(-.74)*	28 *(-.74)*	10 *(-.72)*	25 *(-.66)*	24 *(-.15)*	8 *(-.42)*	8 *(-2.9)*	7 *(-1.68)*	3 *(-1.55)*	3 *(-2.4)*	65 *(.41)*	135 *(1.1)*
P6	M	16	24 *(-.0)*	20 *(-1.48)*	16 *(.22)*	22 *(-1.0)*	24 *(-.15)*	7 *(-.95)*	11 *(.1)*	*21 (.19)*	7 *(-.26)*	5 *(-.4)*	75 *(.82)*	150 *(1.65)*
P7	M	16	14 *(-.74)*	28 *(-.74)*	8 *(-1.03)*	25 *(-.66)*	19 *(-1.43)*	5 *(-2.0)*	7 *(-3.9)*	12 *(-1.01)*	5 *(-.9)*	4 *(-1.4)*	87 *(1.33)*	154 *(1.79)*
P8	M	16	39 *(1.09)*	45 *(.71)*	21 *(1.0)*	30 *(-.08)*	27 *(.62)*	10 *(.63)*	12 *(1.1)*	13 *(-.88)*	9 *(.39)*	5 *(-.4)*	32 *(-.97)*	85 *(-.7)*
P9	M	14	*27 (.21)*	32 *(-.4)*	18 *(.53)*	26 *(-.54)*	21 *(-.92)*	8 *(-.42)*	11 *(.1)*	*21 (.19)*	7 *(-.26)*	5 *(-.4)*	52 *(-.13)*	105 *(.02)*
P10	M	14	19 *(-.37)*	22 *(-1.26)*	9 *(-.88)*	24 *(-.77)*	18 *(-1.69)*	7 *(-.95)*	10 *(-.9)*	17 *(-.35)*	7 *(-.26)*	4 *(-1.4)*	94 *(1.62)*	165 *(2.19)*
P11	M	11	26 *(.14)*	22 *(-1.26)*	16 *(.22)*	24 *(-.77)*	20 *(-1.18)*	7 *(-.95)*	10 *(-.9)*	*15 (-.61)*	6 *(-.58)*	4 *(-1.4)*	80 *(1.03)*	151 *(1.68)*
P12	M	12	13 *(-.81)*	23 *(-1.17)*	12 *(-.41)*	22 *(-1.0)*	19 *(-1.43)*	5 *(-2.0)*	8 *(-2.9)*	12 *(-1.01)*	5 *(-.9)*	4 *(-1.4)*	86 *(1.28)*	153 *(1.75)*
P13	M	16	17 *(-.52)*	28 *(-.74)*	11 *(-.56)*	28 *(-.31)*	21 *(-.92)*	8 *(-.42)*	10 *(-.9)*	14 *(-.75)*	*6 (-.58)*	4 *(-1.4)*	83 *(1.16)*	158 *(1.94)*

Raw scores are reported for each test and participant (see methods). The corresponding normalised values are shown in parenthesis. Normalised z-scores values were computed by subtracting the mean score and dividing by the standard deviation of a reference sample (Al-Joudi et al., 2019). To facilitate inspection of the table, scores better than mean reference performance are underlined. HVLT-R = Hopkins Learning Test – Revised; BVMT-R = Brief Visuospatial Memory Test – Revised; CTT = Colour Trails Test.

Table 3. Patients' lesion anatomy

	Age	Pathology	Lesion laterality	Temporal lobe structures								
				HIP	ERC	PRC	PHC	ITG	MTG	TP	STG	AMG
P1	25	GGs	L	0	+	+	0	0	0	+	0	0
P2	25	MTS	R	++	0	0	0	0	0	+	0	++
P3	50	MG	L	0	0	+	0	0	+	+	0	0
P4	41	GGs	R	0	+	+	0	0	0	+	0	0
P5	31	MTS	R	++	+	0	+	0	+	+	+	++
P6	27	MTS	L	++	0	0	0	0	0	0	0	0
P7	40	MG	L	0	0	0	0	0	+	+	0	0
P8	32	MTS	R	++	0	0	0	+	0	++	0	+
P9	33	MTS	R	++	+	0	++	+	0	0	+	+
P10	22	MTS	L	+	+	0	0	++	0	0	+	0
P11	25	MTS	R	++	+	0	0	0	0	0	+	++
P12	47	GGs	L	0	+	0	0	0	++	++	+	0
P13	32	MTS	R	+	+	0	+	+	0	0	+	0

The table lists the pathology and regions affected by the lobectomy for each patient. Table 3-1 of the extended data shows representative MRI slices through the medial temporal lobe. GG, ganglioglioma; MG, meningioma; MTS, medial temporal sclerosis; HIP, hippocampus; ERC, entorhinal cortex; PRC, perirhinal cortex; PHC, parahippocampal cortex; ITC, inferotemporal cortex; MTG, Middle temporal gyrus; ATP, anterior temporal pole; STG, superior temporal gyrus; AMG, amygdala. ''0'' indicates an unaffected subregion, ''+'' a rostro-caudal lesion extent up to 20 mm, and ''++'' up to 40 mm.

Table 4. Swap errors - analysis of effects

Effects	P(incl)	P(incl|d)	BF_{incl}
B	0.737	0.941	**5.673**
D	0.737	0.925	**4.414**
G	0.737	0.997	**119.755**
B•D	0.316	0.206	0.563
G•B	0.316	0.188	0.500
G•D	0.316	0.891	**17.629**
G•B•D	0.053	0.017	0.317

The table lists each factor and interaction for swap error rates. In the extended data table 4-1 lists the models and associated prior and posterior probabilities from which the values in the present table are computed. P(incl) is the prior probability of the effect; P(incl|d) is the posterior probability of the effect; BF_{incl} *is Bayes factor. A BF greater than 1.0 favours the effect, a BF less than 1.0 favours a null instead. Values of the BF greater than 3.0 are in bold, to highlight those effects that have at least moderate evidence in their favour. Block, probe dimension, group and the interaction of group by probe dimension all have at least moderately strong evidence in their favour.*

Table 5. Generic errors - analysis of effects

Effects	P(incl)	P(incl|d)	BF_{incl}
B	0.737	0.804	1.463
D	0.737	0.815	1.571
G	0.737	0.641	0.637
B•D	0.316	0.142	0.360
G•B	0.316	0.085	0.202
G•D	0.316	0.087	0.206
G•B•D	0.053	7.157e -4	0.013

The table lists each factor and interaction for generic error rates. Table 5-1 of the extended data lists the models and associated probabilities, used to compute the effects. P(incl) is the prior probability of the predictors; P(incl|d) is the posterior probability; BF_{incl} is Bayes factor. A BF greater than 1.0 favours the predictor, a BF less than 1.0 favours a null effect instead. The only predictors with favourable evidence, albeit of very modest entity, are block and probe dimension.